



Experimental and Simulation Results of Wien Bridge Oscillator Circuit Realized with Op-Amp Designed Using a Memristor

İshak Parlar¹ · M. Nuri Almali¹

Received: 28 April 2022 / Accepted: 19 July 2022 / Published online: 3 August 2022
© The Author(s), under exclusive licence to Springer Science+Business Media, LLC, part of Springer Nature 2022

Abstract

In this study, a new op-amp model was created by re-designing the internal structure of the traditional operational amplifier (741 family) circuit element with a linear dopant drift TiO₂ memristor (LDDTM) emulator model. The optimized working conditions and states of this proposed op-amp model were determined. Wien bridge oscillator circuit realized with memristive based op-amp model has been investigated on oscillating start time, settling time, fast fourier transform (FFT) analysis and output parameters. In addition, the efficiency of the wien bridge oscillator circuit realized with a memristor-based opamp has been tested with application circuits and the accuracy and applicability of the proposed memristor-based opamp model has been extensively examined theoretically and supported by experimental and simulation results. Finally, both the simulation and experimental results of the oscillator circuits realized with a memristor-based opamp are presented in detail in tables.

Keywords LDDTM-model · Operational amplifier (op-amp) · Wien bridge oscillator · Fast fourier transform (FFT) · RC oscillators · Oscillator output parameters

1 Introduction

There are many studies in the literature to make the memristor practically usable in analog circuits. These studies were started by Chua in 1971 and continue to the present day [5]. Since the memristor is not widely used as a physical element in the market, emulator circuits continue to be derived [16–18, 20, 23]. In recent years, we see that there are various studies on memristor-based analog oscillators. These studies constitute the transition step to various analog circuits [2, 6].

An oscillator is an electronic device that gives sinusoidal, square, saw and triangle electrical signals in electronic circuits. In other words, it is an electronic element that can generate signals on its own. Oscillations, which are an important parameter of oscillators are electrical signals that change direction, and intensity over time in

electrical-electronic systems [27]. Sometimes oscillations are desirable in analog or digital circuits. To generate sinusoidal or non-sinusoidal signals, major basic structures must be present. These are positive feedback, amplifier element, amplitude limiter and resonant circuit structures. Transistor or operational amplifier can be preferred as amplifier element. For this reason, one of the biggest motivations of the study is to minimize the instabilities in the oscillating start time, settling time and output parameter values in the wien bridge oscillator. It is also the idea to develop the op-amp, which is the main element of oscillator circuits. Traditional op-amps, which have a crucial feature at the feedback point in oscillator circuits, can have a time difference between the input and output responses according to the maximum signal processing speed. This difference affects starting point of oscillation, settling point and stability of the oscillation frequency [21, 24, 25]. The crucial aspects of wien bridge circuit, realized with memristor-based opamp, can be defined as follows:

- It is aimed to improve the frequency, unit, electrical, and switching parameters by transforming the internal structure of the op-amp model which can be redesigned using memristor into an integrated structure with electronic circuit elements.

Responsible Editor: S. Sindia

✉ İshak Parlar
ishakparlar@yyu.edu.tr

M. Nuri Almali
mna1@yyu.edu.tr

¹ Department of Electrical and Electronics Engineering, Van Yuzuncu Yil University, 65080 Van, Turkey

- When the proposed op-amp model is compared with the traditional op-amp model, it is seen that the oscillator start time, settling time, frequency stability and output parameter ranges which are the main problems of RC oscillators, are significantly improved.
- The accuracy and applicability of the proposed op-amp model has been extensively studied theoretically and supported by experimental and simulation results.
- When all parameters are examined and handled one by one, it has been determined that the simulation results are similar to the application results.
- Model parameters that can be preferred according to the purpose of use will shed light on many analog circuit studies that will be created from now on.

The remainder of the paper is arranged into several sections. Section 2 explains the design, configuration, and theoretical analysis of the memristor emulator system, the proposed op-amp model and the wien bridge oscillator circuit. The simulation and experimental results of the wien bridge oscillator realized with the proposed op-amp model provides in detail in Sect. 3. Section 4 draws the main conclusions and future scope of the paper.

2 Materials and Methods

2.1 LDDTM-Emulator Model

Chua's first emulator circuit with memristive behavior consisted of many analog elements [16, 17]. Later, many emulator circuits began to be derived and implemented [12, 13, 18, 20, 23, 26]. The LDDTM-emulator circuit

consisting of a differential amplifier, an integrator circuit and an analog multiplier is shown in Fig. 1.

When an AC voltage is applied between A and B points, the voltage expression on the R_3 resistor is expressed as in Eq. 1.

$$v_{R3} = i(t)R_3 \tag{1}$$

$v_{R3}(t) = v_{in}$ voltage enters the differential amplifier circuit and creates the output voltage v_{U1} . The output voltage of the differential amplifier is shown in Eq. 2.

$$v_{U1} = v_{in} \frac{-R_2}{R_1} = i(t) \frac{-R_3R_2}{R_1} \tag{2}$$

If it is applied to the circuit in Fig. 1, output voltage of the analog multiplier can be calculated as in Eq. 3.

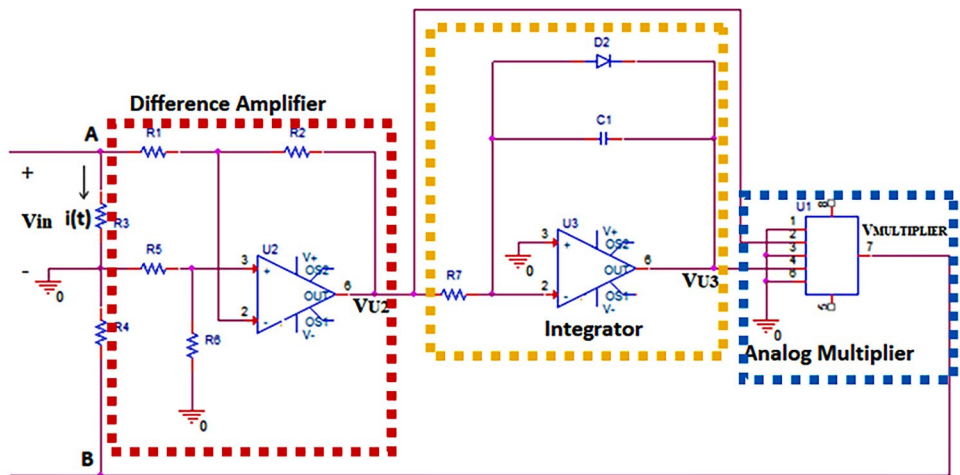
$$v_{MULTIPLIER} = -\left(\frac{R_2R_3}{R_1}\right)^2 \frac{1}{R_7C_1} q(t)i(t) \tag{3}$$

The output voltage of the multiplier is added to the V_{R3} voltage as negative feedback. Thus, the expression for the memristor emulator input voltage or the voltage at the terminals A and B can be given as in Eq. 4.

$$v_{mem} = \left(R_3 - \left(\frac{R_2R_3}{R_1} \right)^2 \frac{1}{R_7C_1} q(t) \right) i(t) \tag{4}$$

Figure 2 shows the hysteresis curve of the emulator circuit at different frequencies. In many emulator circuits, the memristive behavior can be changed by changing the values of active or passive circuit elements [4, 13, 20, 26]. This flexibility can show us that the memristor is not only working at low frequencies but also at higher frequencies.

Fig. 1 LDDTM-emulator circuit diagram



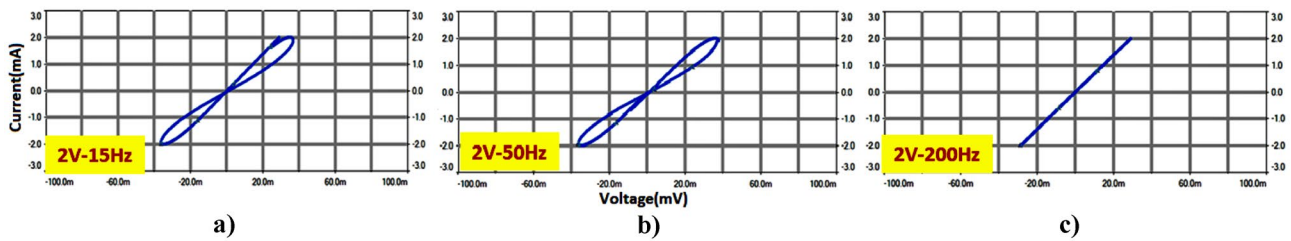


Fig. 2 Hysteresis curves of the emulator fed with sinusoidal voltage at different frequencies; a 15 Hz, b 50 Hz and c 200 Hz

2.2 Configuration and Description of the Proposed Op-Amp Model

In this study, the memristor emulator is integrated with the op-amp as a subsystem. The effects of the memristor Emulator, placed in the op-amp internal circuit on the op-amp's output responses, and specification tests, are discussed in this section. In Fig. 3, the memristor-based opamp created in the PSpice program is shown.

In general, the internal structure of an op-amp consists of 5 basic layers as differential amplifier, bias current, gain, level change, and output layer [8, 9, 11]. The responses of the memristor emulator placed in the op-amp internal circuit were examined one by one in the specified layers and it was seen that the layer giving the optimum output response could be replaced by the R5 resistor in the level change layer.

A voltage difference V_{in} at the op-amp inputs (pins 2 and 3) causes a small differential current $i_{in} \approx V_{in}/(2h_{ie}h_{fe})$ in the bases Q1 and Q2. This differential base current causes a change in differential collector current in each leg by $i_{in}h_{fe}$. When Q1 is entered into the transconductance of $g_m = h_{fe}/h_{ie}$, the current at the base of Q15 can be regulated as in Eq. 5.

$$\begin{aligned}
 V_{in} &= V^+ - V^- \\
 i_{in} &\approx \frac{V_{in}}{2h_{ie}h_{fe}} \approx I_{C11} \\
 I_{B15} &= \frac{V_{in}g_m}{2}
 \end{aligned}
 \tag{5}$$

A current signal I_{B15} at the base of Q15 causes a current in Q19 of order $I_{B15}\beta^2 \approx I_{C19}$. This current signal creates a voltage at the bases Q14/Q20 of the output transistors proportional to the h_{ie} of the respective transistor. If we rearrange Eq. 5 according to emitter and collector currents of Q19 transistor, Eq. 6 is obtained [3, 9, 10, 14].

$$I_{E19} \approx I_{C19} \approx \underbrace{\frac{V_{in}g_m}{2}}_{I_{B15}} \beta^2
 \tag{6}$$

The resistor (39KΩ) connecting Q11 and Q12, and the given supply voltage ($V_{S+} - V_{S-}$ determines the current in the current mirrors (matched pairs) Q10/Q11 and Q12/Q13. Collector current of Q11 is found as Eq. 7.

$$I_{C11} \times 39K = V_{S+} - V_{S-} - 2V_{BE}, V_S = \pm 20V
 \tag{7}$$

The constant current in Q11/Q12 (as well as Q13) will be $\approx 1mA$. For a typical 741 of about 2mA, a supply current dominates the quiescent supply current of these two bias currents [3]. In this circuit, if the collector current of Q11, which is obtained by placing a memristor emulator circuit instead of 39KΩ, is rearranged using the memristor emulator circuit equation given in Eq. 5, Eq. 8 is obtained.

$$\begin{aligned}
 I_{C11} \times M(q) &= V_{mem} = V_{S+} - V_{S-} - 2V_{BE}, V_S = \pm 20V \\
 I_{C11} &= \frac{V_{mem}}{\left(R_3 - \left(\frac{R_2 R_3}{R_1} \right)^2 \frac{1}{R_7 C_1} q(t) \right)} i_{mem} \approx I_{C11}
 \end{aligned}
 \tag{8}$$

Then the output voltage expression can be derived as in Eq. 9.

$$\begin{aligned}
 V_{out} &= |V_{BE14} - V_{BE20}| + R_{50\Omega} I_{E20} - R_{25\Omega} (\beta I_{B14} - I_{B17}) \\
 V_{out} &= |V_{BE14} - V_{BE20}| + R_{50\Omega} I_{E20} - R_{25\Omega} (\beta (I_{C11} - I_{B16} - I_{C17}) - I_{B17})
 \end{aligned}
 \tag{9}$$

Equation 10 can be obtained by placing the memristor current and voltage expressions in Eq. 9 by making use of Eq. 8 [19].

$$V_{out} = |V_{BE14} - V_{BE20}| + R_{50\Omega} I_{E20} - R_{25\Omega} \left(\beta \left(\frac{V_{mem}}{\left(R_3 - \left(\frac{R_2 R_3}{R_1} \right)^2 \frac{1}{R_7 C_1} q(t) \right)} - I_{B16} - I_{C17} \right) - I_{B17} \right)
 \tag{10}$$

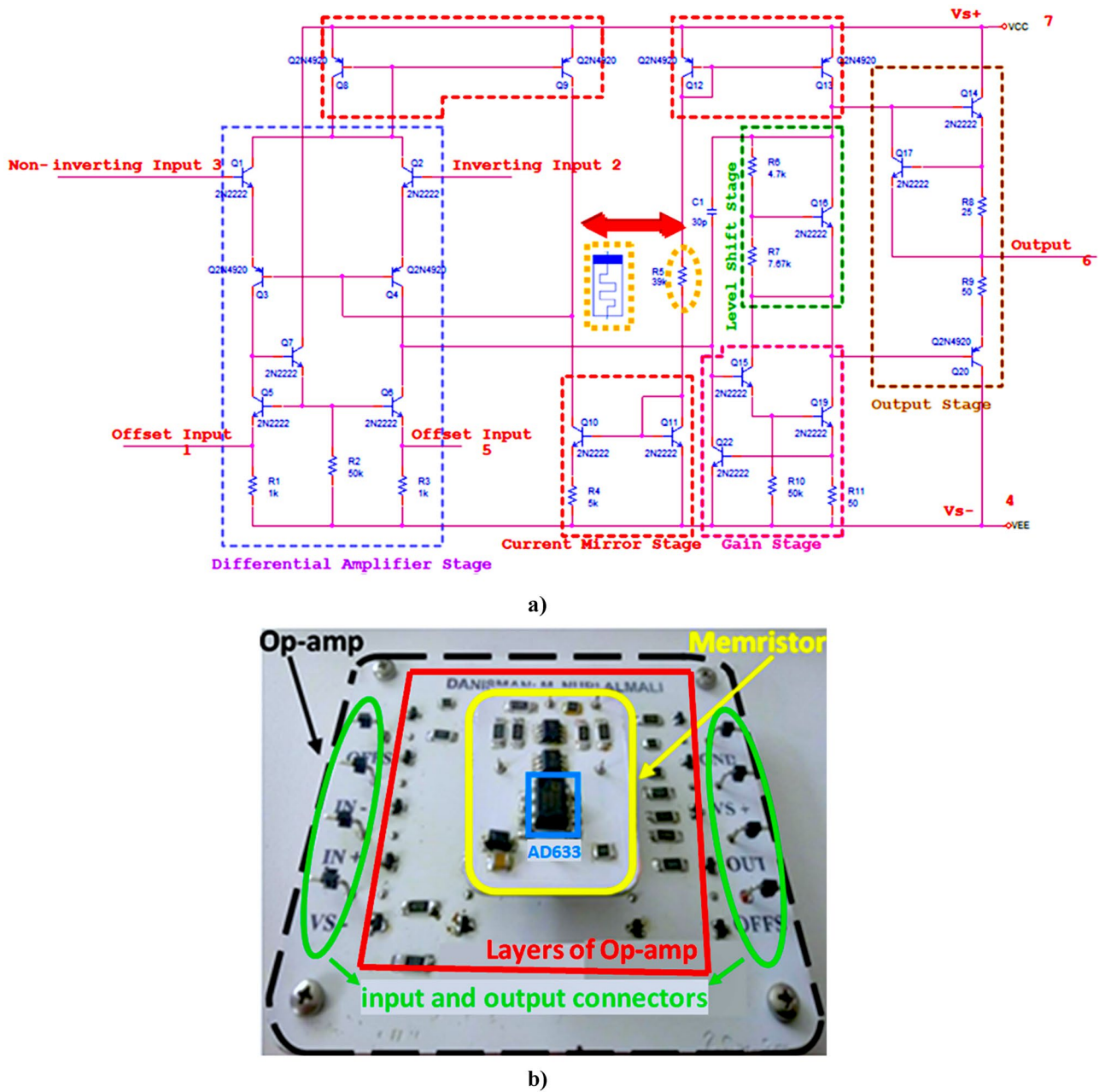


Fig. 3 a Memristor-based opamp circuit, b Experimental setup of memristor-based opamp

2.3 Wien Bridge Oscillator

Figure 4, shows the op-amp and the wien bridge oscillator scheme designed using a memristor. Numerical analyzes of the proposed circuit are given below, respectively.

When the protective structure for the wien bridge oscillator is neglected, the transfer function can be expressed as Eq. 11;

$$\frac{V_i}{V_o} = \frac{R_2 // \frac{1}{C_2 s}}{R_1 + \frac{1}{C_1 s} + R_2 // \frac{1}{C_2 s}} = \frac{\frac{R_2}{1 + R_2 C_2 s}}{\frac{1 + R_1 C_1 s}{C_1 s} + \frac{R_2}{1 + R_2 C_2 s}} \tag{11}$$

If analyzes are made by passing from the *s* plane to the *jw* plane;

$$\frac{V_i}{V_o} = T(s) = \frac{R_2 C_1 jw}{1 - R_1 R_2 C_1 C_2 w^2 + (R_1 C_1 + R_2 C_2 + R_2 C_1) jw} \tag{12}$$

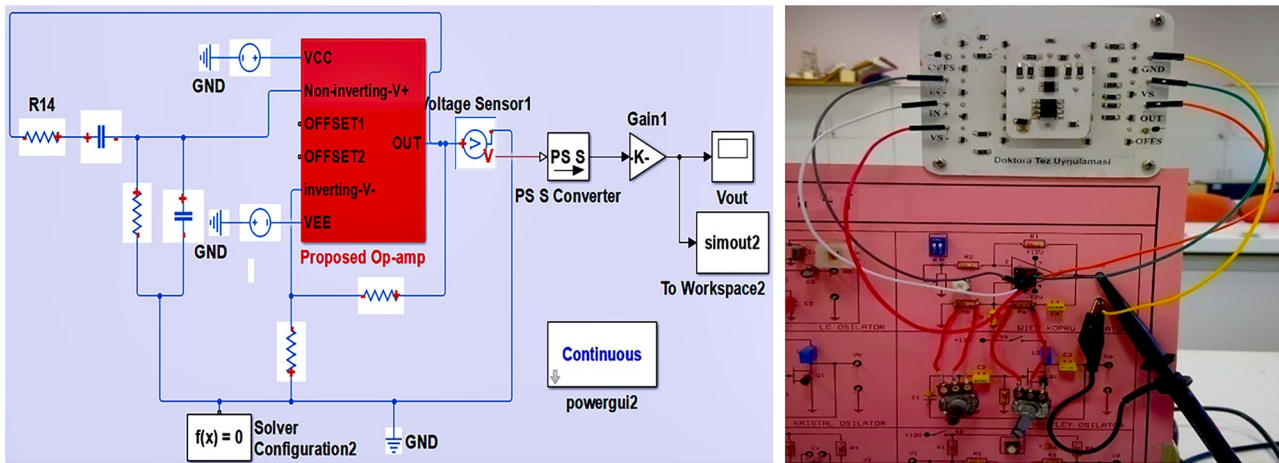


Fig. 4 The wien bridge oscillator circuit realized with the proposed op-amp; **a** simulation scheme and **b** experimental set

$1 - R_1R_2C_1C_2\omega^2$ must be equal to zero, since the total phase shift must be zero according to the Barkhausen stability criterion to obtain the required oscillations. Wien bridge oscillators are designed by choosing $R_1 = R_2 = R$ and $C_1 = C_2 = C$. In this case, the oscillation frequency can be calculated as follows.

$$\omega = \frac{1}{\sqrt{R_1R_2C_1C_2}} \rightarrow f = \frac{1}{2\pi RC} \tag{13}$$

If the oscillation condition for the closed loop gain is written as in Eq. 14;

$$\frac{V_i}{V_o} = \frac{R_4R_5 + R_3R_4}{R_3R_4 + R_3R_5 + R_4R_5} = 0.34 \tag{14}$$

available as. From here, it is expressed as $R_3/R_4 \approx 2.12$ oscillation condition.

3 Results

The output responses of the wien bridge oscillator circuit at the same oscillation frequency, according to the changing $R_{mem}(q)$ in the op-amp circuit designed using a memristor are shown in Fig. 5.

It has been observed that the proposed op-amp model, based on the oscillation start and oscillation band settling times at mid-frequencies, these times are shorter than the traditional op-amp model. Also, in Fig. 6, the frequency responses of both op-amp models in the mid-frequency region for the wien bridge oscillator circuit are discussed.

Wien bridge oscillator circuits realized using memristor-based opamp and traditional op-amp respectively, are investigated not only in the mid-frequency regions but also in the low and high frequency regions. Experimental and simulation results in all frequency regions are compared in detail in Table 1. Improvements can be seen especially in the high frequency regions.

4 Discussion

In order to measure the performance and efficiency of the proposed op-amp model, wien bridge oscillator circuits [1, 7, 15, 22, 28], which are RC oscillators, are preferred. Both simulation models and experimental models of the proposed op-amp model and traditional op-amp models were carried out on wien bridge oscillator circuit. According to different op-amp models, the fundamental frequency of the wien bridge oscillator circuit simulations was found to be 3120 Hz for traditional op-amp simulation and approximately 3058 Hz for the proposed op-amp simulation model. The 1.98% difference in fundamental frequencies is due to the op-amp's unpredictable simulation parameters. Parameters such as the selection of the ODE function, the sensitivity of the simulation step size, the initial values of passive circuit elements such as capacitors and diodes used in the circuit, and the beta points of transistors may adversely affect the operation of the system. It has been observed that the wien bridge oscillator simulation model realized with a memristor-based opamp starts to oscillate approximately 72.22% earlier than the traditional op-amp model. The reason for this is the convergence parameters

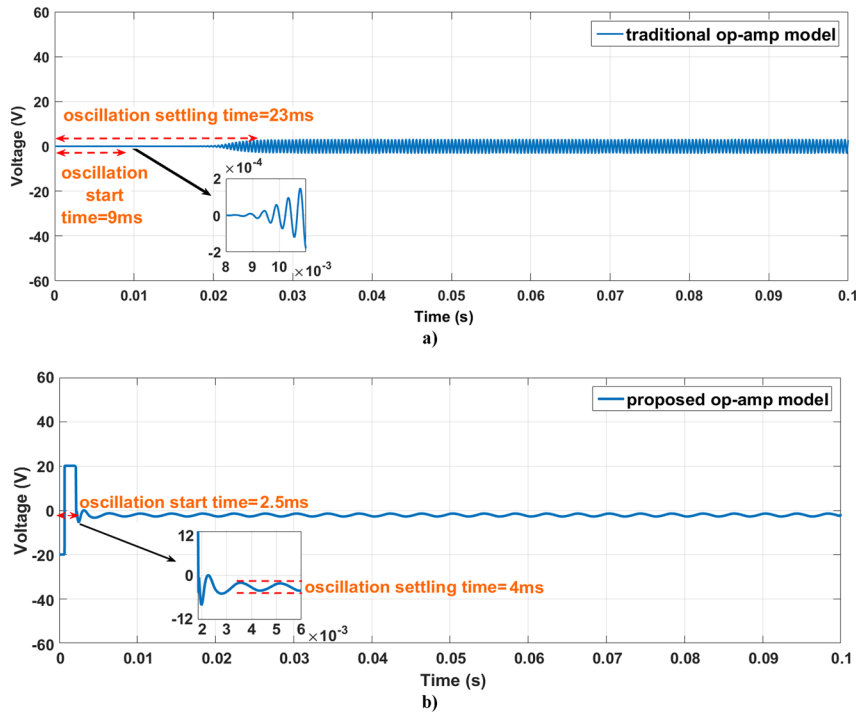


Fig. 5 Oscillation start and settling times of wien bridge oscillator circuit realized with different op-amp models; **a** traditional op-amp model (simulation result), **b** proposed op-amp model (simulation result), **c** tra-

ditional op-amp model (experimental result), and **d** proposed op-amp model (experimental result)

of the Matlab/Simscape program used in the simulation. These parameters are generally solver, limit data points, refine factor and number of consecutive zero crossings. Also, there was an improvement of 82.60% in the oscillation band settling times. Likewise, it has been observed that there are significant improvements in the setting times

in the experimental models compared to the traditional op-amp model. In addition, on wien bridge oscillator of the proposed op-amp and traditional op-amp models, not only the mid-frequency region, but also the lowest and highest frequency regions where they can operate have been determined. It has been calculated that the frequency

Fig. 6 FFT responses of wien bridge oscillator realized with different op-amp models (at nominal test conditions); **a** traditional op-amp (simulation) and **b** proposed op-amp (simulation) ($R_1 = R_2 = 51K\Omega, C_1 = C_2 = 1nF$)

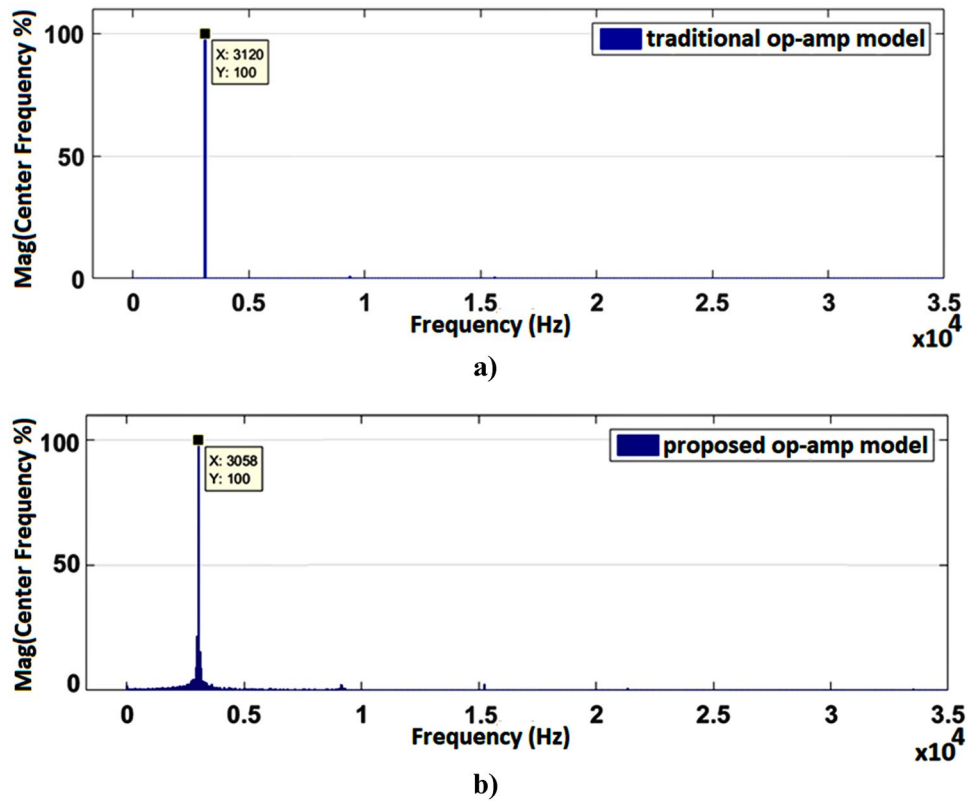


Table 1 Characteristic analysis values of the proposed op-amp and traditional op-amp models on the wien bridge oscillator

Oscillator type		Frequency range											
		Low (Hz)				Middle (KHz)				High (MHz)			
		4	8	10		3	4		0.811	1.62			
Traditional wien bridge	Simulation	×	✓	✓	✓	✓	✓	✓	✓	✓	✓	✓	✓
	Experimental	×	×	✓	✓	✓	✓	✓	✓	✓	✓	×	×
Proposed wien bridge	Simulation	×	✓	✓	✓	✓	✓	✓	✓	✓	✓	✓	×
	Experimental	×	×	×	✓	✓	✓	✓	✓	✓	✓	✓	×

regions where wien bridge oscillator can operate with the proposed op-amp model expand and these regions are presented in detailed table.

As a result, the complexity of the internal structure of the proposed op-amp model, capacitive effects, Miller effects, unpredictable factors and parameters not specified in the manufacturer's catalogs were the most important challenges. It is predicted that such challenges will be minimized by using optimization methods. When all parameters are examined and handled one by one, it has been determined that the simulation results are similar to the experimental results. Thanks to the model parameters that can be preferred according to the purpose of users, the proposed op-amp model will shed light on many analog circuits.

Authors' Contributions İshak Parlar: Writing-Reviewing and Editing, Conceptualization, Methodology, Visualization, Investigation. M. Nuri Almalı: Supervision, Writing- Original draft preparation, Validation, Writing- Original draft preparation, Data curation.

Funding This research did not receive any specific grant from funding agencies in the public, commercial or not for profit sectors.

Availability of Data and Material Authors declare the transparency of the data used in their articles.

Declarations

Conflicts of Interest and Competing Interests The authors report there are no competing interests to declare.

References

- Abuelma'atti MT, Khalifa ZJ (2016) A memristor-based Wien-bridge sinusoidal/chaotic oscillator. *Int J Electr Eng Educ* 53(3):280–288. <https://doi.org/10.1177/0020720915622471>
- Barbarosou M, Paraskevas I, Kliros G, Andreatos A (2017) Implementing transistor roles for facilitating analysis and synthesis of analog integrated circuits. *Proc Global Engineering Education Conference (EDUCON)* 423–430. <https://doi.org/10.1109/EDUCON.2017.7942881>
- Boylestad RL, Louis N (2015) *Electronic Devices and Circuit Theory*, Palme Publishing, 10th Edition, Ankara
- Chilukuri M, Jung S (2015) A high frequency memristor emulator circuit. *Proc. IEEE Dallas Circuits and Systems Conference (DCAS)*, 1–4. <https://doi.org/10.1109/DCAS.2015.7356594>
- Chua L (1971) Memristor-the missing circuit element. *IEEE Transactions on Circuit Theory* 18(5):507–519. <https://doi.org/10.1109/TCT.1971.1083337>
- Elsamman AH, Radwan AG, Madian AH (2014). Resistorless memristor based oscillator. *Proc. 26th International Conference on Microelectronics (ICM)* (168–171). <https://doi.org/10.1109/ICM.2014.7071833>
- He F, Ribas R, Lahuec C, Jézéquel M (2009) Discussion on the general oscillation startup condition and the Barkhausen criterion. *Analog Integr Circ Sig Process* 59(2):215–221. <https://doi.org/10.1007/s10470-008-9250-1>
- Huijsing JH (1993) Design and applications of the operational floating amplifier (OFA): The most universal operational amplifier. *Analog Integr Circ Sig Process* 4(2):115–129. <https://doi.org/10.1007/BF01254863>
- Information D, Schematic S (2018) μ A741 general-purpose operational amplifiers, Texas Instruments.
- Jung W (2005) *Op-Amp applications handbook*. Newnes
- Kapil A, Shah A, Agarwal R, Sharma S (2012) Analysis and comparative study of different parameters of operational amplifier using bipolar junction transistor and complementary metal oxide semiconductor using tanner tools. *Int J Soft Comput Eng* 2 (5), 19– 23. ISSN: 2231–2307
- Kim H, Sah MP, Yang C, Cho S, Chua LO (2012) Memristor emulator for memristor circuit applications. *IEEE Trans Circuits Syst I Regul Pap* 59(10):2422–2431. <https://doi.org/10.1109/TCSI.2012.2188957>
- López-Sánchez C, Carrasco-Aguilar MA, Muñiz-Montero C (2015) A 16Hz–160kHz memristor emulator circuit. *AEU Int J Electron Commun* 69(9):1208–1219. <https://doi.org/10.1016/j.aeue.2015.05.003>
- Mancini R (2003) *Op amps for everyone: design reference*. Newnes
- Mehta H, Agarwal N, Dutt K, Jain S (2013) Effect of Current Feedback Operational Amplifiers using BJT and CMOS. *International Journal of Advanced Research in Computer Science and Software Engineering* 3(4):1081–1087. <https://doi.org/10.6088/ijacit.22.10002>
- Mutlu R, Karakulak E (2018) Memristor-based phase shifter. *Proc. 2nd International Symposium on Multidisciplinary Studies and Innovative Technologies (ISMSIT)* 1–5. <https://doi.org/10.1109/ISMSIT.2018.8567280>
- Mutlu R, Karakulak E (2009) A memristor (Memory Resistor) emulator circuit that can be used in engineering education. *Proc. Electrical Electronics Computer Engineering Education Symposium*
- Muthuswamy B (2010) Implementing memristor based chaotic circuits. *Int J Bifurcation Chaos* 20(5):1335–1350. <https://doi.org/10.1142/S0218127410026502>
- Parlar I, Almali MN (2022) Comparison of the output parameters of the memristor-based op-amp model and the traditional op-amp model. *J Electron Test* 38(2):131–143. <https://doi.org/10.1007/s10836-022-05991-3>
- Ranjan RK, Sagar S, Roushan S, Kumari B, Rani N, Khateb F (2019) High-frequency floating memristor emulator and its experimental results. *IET Circuits Devices Syst* 13(3):292–302. <https://doi.org/10.1049/iet-cds.2018.5191>
- Robinson FNH, Ockendon H (1998) A pure sine-wave oscillator with a fast settling time. *Eur J Appl Math* 9(2):95–104. <https://doi.org/10.1017/S095679259800343X>
- Sharma VK, Ansari MS, Joshi AM (2017) Memristor-based high performance third order quadrature oscillator. *Proc. TENCON 2017-IEEE Region 10 Conference* 2949–2954. <https://doi.org/10.1109/TENCON.2017.8228367>
- Sözen H, Çam U (2015) New memristor emulator circuit using OTAs and CCII. *Proc. 9th International Conference on Electrical and Electronics Engineering (ELECO)* 10–14. <https://doi.org/10.1109/ELECO.2015.7394456>
- Toker A, Çiçekoğlu O, Kuntman H (2002) On the oscillator implementations using a single current feedback op-amp. *Comput Electr Eng* 28(5):375–389. [https://doi.org/10.1016/S0045-7906\(00\)00059-8](https://doi.org/10.1016/S0045-7906(00)00059-8)
- Tsuzuki Y, Adachi T, Zhang JW (1995) Fast start-up crystal oscillator circuits. *Proc. International Frequency Control Symposium (49th Annual Symposium)* 565–568. <https://doi.org/10.1109/FREQ.1995.484055>
- Vista J, Ranjan A (2019) A simple floating MOS-memristor for high-frequency applications. *IEEE Transactions on Very Large Scale Integration (VLSI) Systems* 27 (5), 1186–1195. <https://doi.org/10.1109/TVLSI.2018.2890591>
- Westra JR, Verhoeven CJ, Van Roermund AH (2000) *Oscillators and Oscillator Systems*. Kluwer
- Yumrukaya E (2017) *Analysis and Design of Oscillator Circuits Using Memristors* (Master's Thesis, unpublished). Dokuz Eylul University, Institute of Science and Technology, Izmir, Turkey

Publisher's Note Springer Nature remains neutral with regard to jurisdictional claims in published maps and institutional affiliations.

Springer Nature or its licensor holds exclusive rights to this article under a publishing agreement with the author(s) or other rightsholder(s); author self-archiving of the accepted manuscript version of this article is solely governed by the terms of such publishing agreement and applicable law.

İshak Parlar graduated from Department of Electrical and Electronics Engineering, Gazi University (Ankara, Turkey) in 2010. He completed M.Sc. degree at Yuzuncu Yil University (Van, Turkey) in 2018. He continues Ph.D. research at Yuzuncu Yil University (Van, Turkey). Currently, he is a Research Assistant in Department of Electrical and Electronics Engineering at Yuzuncu Yil University. His research interests are application of analog electronics, memristor design, experimental emulators, encrypted communication, chaos, synchronization, application of biomarkers (ECG, EMG, EEG, etc.) and digital electronics applications.

M. Nuri Almali received the B.Sc. degree from Karadeniz Technical University (Trabzon, Turkey) and M.Sc. and the Ph.D. degrees from Yuzuncu Yil University (Van, Turkey). Currently, he is working as an Associate Professor in Department of Electrical and Electronics Engineering at Yuzuncu Yil University. His research interests are digital electronics, basic electronics, encrypted communication, chaos, synchronization and optimization algorithms.